School of Biosciences

FINAL YEAR PROJECT REPORT
2020-21

TITLE: Co-occupying Swi/Snf and Ssn6-Tup1 chromatin remodelling activities are required for full nucleosome free region accessibility at Ssn6 promoter targets

STUDENT NUMBER: C1802134

DEGREE: Biological Sciences (BSc)

TYPE OF PROJECT: Practical Project (Bioinformatics)

WORD COUNT (Summary): 333

WORD COUNT (Main Body): 5 050

ABSTRACT

Background: By altering nucleosome positioning and structure, eukaryote co-activator and co-repressor remodelling factors change the structure of chromatin to positively and negatively regulate gene expression respectively. Swi/Snf and Ssn6-Tup1 complexes are such factors whose distinct binding and co-occupancy has been identified as a requirement for repressive chromatin structure remodelling at promoter regions and upstream domains. Micrococcal nuclease (MNase) directed chromatin particle spectrum analyses offer an opportunity to map nucleosome landscapes throughout the Saccharomyces cerevisiae genome at a range of specified features.

Materials and Methods: MNase digested DNA was sequenced from Ssn6 knockout (*Ssn6Δ*), Snf2 knockout (*Snf2Δ*) and *Snf2*/*Ssn6* double knockout (*Snf2ΔSsn6Δ*) mutant S. cerevisiae strains providing 150bp nucleosomal paired reads for processing by a suite of Perl executable scripts. Chromosomal nucleosome distributions were visualised in the Integrated Genome Browser by plotting nucleosome frequency against genomic positions. Typical nucleosome occupancies were determined for a range of genomic features by plotting normalised cumulative nucleosome frequency distributions and clustered into common occupancy patterns using Cluster 3.0.

Results: Insert size distribution chromatin particle size classes reflect input MNase-digested DNA size spectra for WT and *Ssn6Δ* bio-replicates and, among samples, bio-replicates correlate very strongly. A Ty1 retrotransposon duplication event (chrIV:1 101 332-1 206 996) was described by apparent abnormal nucleosome frequency that results in no change to typical retrotransposon gene nucleosome occupancy. Nucleosome occupancy data provide evidence suggesting regulatory interactions between Ty1 duplication and tRNA gene expression. Swi/Snf and Ssn6-Tup1 co-occupancy leads to the most accessible NFR formation at Ssn6 binding promoter regions and ChIP-exo Ssn6 binding regions. This finding was reflected in nucleosome positioning at hexose transporter encoding gene *HXT2* and *HXT7* promoter regions.

Conclusions: Further studies on Ssn6-Tup1 chromatin remodelling activity should include sequence tagged Ty1 elements to identify Ty1 insertion sites and consider this against tRNA gene nucleosome occupancy. Co-occupying Swi/Snf and Ssn6-Tup1 chromatin structure remodelling is transcriptionally activating by increased NFR accessibility at Ssn6 binding promoter regions. Despite evident Ssn6-Tup1 repression, *HXT2* and *HXT7* loci experience these co-occupying effects demonstrating a remodelling opposing interplay.

INTRODUCTION

Chromatin remodelling at the nucleosome level is central to gene expression regulation

There are chromatin phase spectra of more and less densely packed structures that influences the spatial arrangement and transcriptional activity of the eukaryotic genome (Voong et al. 2017). The fundamental particle of chromatin is a nucleoprotein complex known as the nucleosome. Comprising a histone protein octameric core wrapping 147 base pairs (bp) and 1.65 super helical turns of DNA, nucleosomes appear cytologically rigid yet function highly dynamically (Venkatesh and Workman 2015). A nucleosome determines, by steric occlusion, the accessibility of its wrapped DNA to a range DNA binding protein (DBPs). Occluded DNA is protected from DBP activity including that of the RNA polymerase complex as well as sequence specific transcription factors. Therefore, the positioning of a nucleosome contributing to overall nucleosome occupancy at a specified locus is a key regulatory step in active gene transcription and silent gene repression. Numerous remodelling factors with the capacity for interdependent interaction are required for the modulation of nucleosome positioning as to positively or negatively regulate transcription.

Co-activators remodel nucleosomes to positively modulate gene expression regulation

Broadly, remodelling factors may be co-activator or co-repressor complexes that possess the ability to alter nucleosomes in position and/or structure utilising the energy of ATP hydrolysis (Tsukiyama 2002). Such co-activators or co-repressors are the multiunit ATP-dependant chromatin remodelling factors that contain an ATPase subunit belonging to the Swi2/Snf2 ATPase superfamily (Eisen et al. 1995). Four different ATPase subunit classes have been described: SWI/SNF, ISWI, CHD and INO80 (Tsukiyama 2002). There are five members of the SWI/SNF class and, in particular, the eponymous Swi/Snf complex contains the Swi2/Snf2 ATPase subunit. The *in vitro* biochemical activities of Swi/Snf have been investigated to reveal its ability to slide and displace nucleosomes (Whitehouse et al. 1999), twist DNA (Havas et al. 2000) and disrupt the nuclease digestion pattern of nucleosomes (Logie and Peterson 1997). Using the *Saccharomyces cerevisiae* as a model organism, *in vivo* studies show the functions of Swi/Snf include facilitating the activation of inducible genes (Winston and Carlson 1992) and its formation of an open chromatin structure (Hirschhorn et al. 1992). Although there is evidence for its negative regulation of transcription in multiple genes (Sudarsanam et al. 2000), Swi/Snf and its constituent Swi2/Snf2 ATPase subunit is considered a co-activator complex that alters nucleosome positioning to positively regulate transcription and gene expression. Notably, a range of cancers exhibit a high frequency of mutations in genes encoding subunits of the human ortholog Swi/Snf complexes (Mittal and Roberts 2020).

Co-repressors remodel nucleosomes to negatively modulate gene expression regulation

The Ssn6-Tup1 (also known as Cyc8-Tup1) complex is one of the earliest identified co-repressor complexes in *S. cerevisiae*. In higher eukaryotes, the Tup1 subunit is related in its C terminal domain to the Groucho family of co-repressors (Courey and Jia 2001). The complex plays a role in a range of pathways including glucose, starch and oxygen utilisation, DNA repair and meiosis (Malave and Dent 2006). The long-range chromatin remodelling activities of Ssn6-Tup1 is evidenced to be associated with that of Swi/Snf (Fleming and Pennings 2007; Fleming et al. 2014). Recently, Fleming et al. (2014) investigated the Ssn6-Tup1 mechanism of action on one of its known repressive target genes, *S. cerevisiae FLO1*. Ssn6-Tup1 cooperated with histone deacetylases (HDACs) Hda1p and Rpd3p to robustly repress *FLO1*. Furthermore, the occupancy of the HDACs and Swi/Snf decreased and increased in parallel respectively in the absence of Ssn6-Tup1. The data indicate that Ssn6-Tup1 and Swi/Snf bind distinctly, and this is required for the long-range remodelling of the *FLO1* promoter as well as upstream chromatin. Previous work on chromatin remodelling activities of Ssn6-Tup1 focussed on the contribution of the Ssn6 and Tup1 subunits and used deletion mutants of each subunit (Fleming et al. 2014). As such, the chromatin remodelling interplay between Ssn6-Tup1 and Swi/Snf are yet to be entirely resolved.

Micrococcal nuclease sequencing for nucleosome occupancy analyses

Micrococcal nuclease sequencing (MNase-seq) is a nuclease protection assay that maps individual nucleosomes throughout a genome. Endo-exonuclease MNase preferentially degrades the linker DNA found between nucleosomes while nucleosomal DNA is not accessible to the nuclease's digestion. As such, DNA wrapped by chromatin particles remain undigested and can be subject to massively parallel sequencing. MNase mapping experiments involve cell permeabilization, nuclei isolation, MNase digestion and undigested DNA purification (Voong et al. 2017). By sequencing the processed chromatin particle DNA fragments, the resultant MNase-seq read data can be utilised in a range of analyses that investigate nucleosome positioning and occupancy *in vivo*. As the data is derived from a cell population, nucleosome positioning is interpretated as a frequency distribution where the height of a given peak indicates the approximate probability of a nucleosome being present at the corresponding genomic position across all cells. Consequently, the 'strength' of the nucleosome position is visualised.

The Swi/Snf Ssn6-Tup1 chromatin remodelling interplay at tRNA gene and SSN6 bound loci

This study aimed to further resolve the co-occupying interactions of Swi/Snf and Ssn6-Tup1 complexes in chromatin remodelling and their effect on gene expression regulation throughout the genome by comparing differing *SSN6* and *SNF2* status MNase-seq datasets in a chromatin particle spectrum analysis (Kent et al. 2011). Confirmed Ssn6 subunit binding genomic features were used to infer the Swi/Snf role at genomic features targeted by Ssn6-Tup1 chromatin remodelling and, further, to determine whether the two complexes' interactions throughout the remodelling targets of Ssn6-Tup1 are unanimous with that of the *FLO1* promoter region. To this end, typical nucleosome occupancy was examined at global Ssn6 binding loci and Ssn6 binding promoter regions for *SSN6* knockout (*Ssn6Δ*), *SNF2* knockout (*Snf2Δ*) and *SNF2*/*SSN6* double knockout (*Snf2ΔSsn6Δ*) mutant *S. cerevisiae* strains. In addition, occupancy was investigated at Ty1 retrotransposon associated gene loci and tRNA gene loci. Utilising normalised cumulative frequency plots (CFDs) of 150bp paired reads, typical nucleosome occupancy profiles of specified genomic features show their common chromatin patterns including nucleosome free regions (NFRs) and nucleosomes of weak and strong positioning. Of note is the previously described Ssn6 mutation Y353C which leads to the transcriptional upregulation of hexose transporter encoding genes (Nijland et al. 2017). In particular, increased expression of the 'main' hexose transporters such as *HXT2* and *HXT7*. Here, these model gene loci provide an *in situ* insight into alternative mechanisms of Swi/Snf and Ssn6-Tup1 remodelling mediated gene expression regulation. In whole, the study provides evidence of a balance in transcriptionally

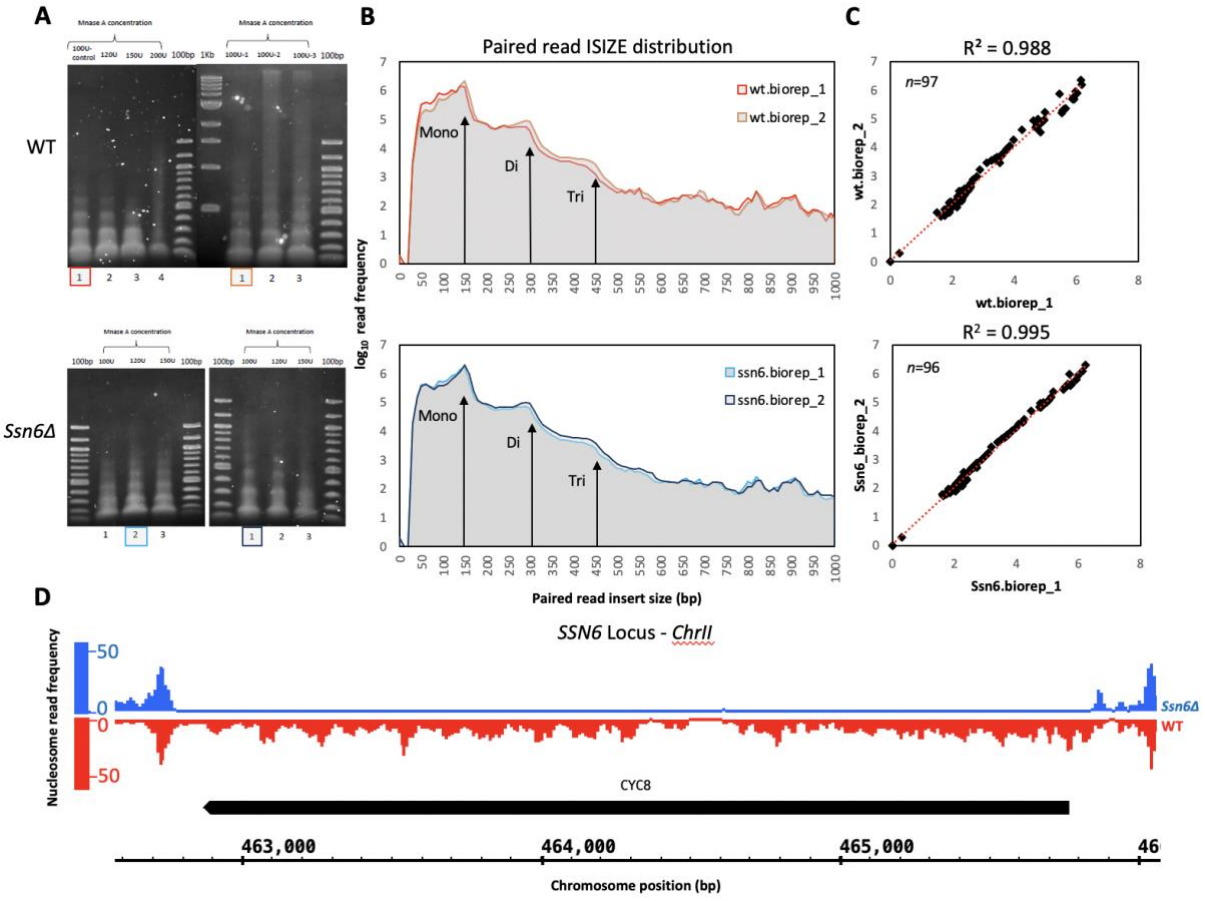

Figure 1 WT and *Ssn6Δ* paired read insert size distributions are consistent between bio-replicates and *ChrII* nucleosome frequency distribution confirms *SSN6* deletion. A MNase-digested DNA agarose gel electrophoresis shows chromatin particle size spectra. WT and *Ssn6Δ* bio-replicates are indicated red, orange and light blue, dark blue respectively. **B** Mono-, Di- and tri-nucleosome peaks reflect the size spectra and provide 150bp nucleosomal paired reads. Insert size (ISIZE) $\log_{10}$ read frequency (Y axis) distributions were plotted for WT and *Ssn6Δ* samples by end-to-end distances of paired sequence reads (X axis). **C** Bio-replicate ISIZE distributions corelate very strongly for both WT and *Ssn6Δ*. R^2-values refer to correlation coefficient of bio-replicates. **D** *SSN6* (*CYC8*) knockout visualisation by nucleosome distribution, displayed using the S288C strain 2011 SacCer 3 genome.

repressive and activating chromatin structure remodelling by co-occupying Swi/Snf and Ssn6-Tup1 at individual promoters targeted by Ssn6 binding.

MATERIALS AND METHODS

Yeast culture and MNase chromatin digestion

Budding yeast wild-type reference strain BY4742 (*Saccharomyces cerevisiae*, genotype: *MATa; his3Δ1; leu2Δ0; lys2Δ0; ura3Δ0*) was obtained from EUROSCARF. Prof. Alastair Fleming and Dr. Mohamed Alhussain at The Moyne Institute, Trinity College Dublin made *SSN6* and *SNF2* deletions for mutant strains using standard gene replacement methods (Wach et al. 1994). Dr. Mohamed Alhussain carried out yeast culturing and MNase chromatin digestion in a published method (Kent et al. 2011) originally described by Kent and Mellor (1995). For yeast strain growth, a rich media (YPD - 1% w/v yeast extract, 1% w/v Bacto Peptone and 2% w/v dextrose) was used. At mid-log phase, cell walls were removed enzymatically to produce sphaeroplasts and permeabilised using NP-40 detergent. Chromatin was partially digested by treating yeast cells with 100 - 120u/ml of MNase A and proteinase K treatment at 50°C, phenol extraction and alcohol precipitation purified the MNase-digested DNA. Following this, the chromatin fractions were separated by agarose gel electrophoresis to produce a DNA ladder of chromatin particle size spectra.

MNase-digested DNA sequencing and alignment

Within the Cardiff School of Biosciences Genomics Research Hub, DNA sequencing libraries were prepared using the NEXTFLEX Rapid kit (Bioone/Perkin Elmer) and sequenced on an Illumina NextSeq500 in 50bp paired-end mode. A total of four paired read sequencing yields comprise the WT and *Ssn6Δ* samples: 49 255 791 (WT bio-replicate 1), 33 721 698 (WT bio-replicate 2), 44 573 513 (*Ssn6Δ* bio-replicate 1) 44 871 736 (*Ssn6Δ* bio-replicate 2).

Paired read alignments and their output manipulation were carried out at the command line level. Bowtie 1 (Langmead et al. 2009) was used for aligning each bio-replicate to the 2011 SacCer 3 genome. By trimming paired reads to 36bp, Bowtie removed anomalous adapter sequence tracts which failed to align. Consequently, overlapping read pairs could be returned from relatively short input, nuclease protected DNA species. Paired reads were input in FASTQ format, and their subsequent alignments were output as SAM format. SAMtools (Li et al. 2009) was used for sorting paired read alignments into chromosome order.

Paired read insert size and nucleosome frequency distribution analyses

Frequency distributions from chromosome-ordered SAM bio-replicate alignments were plotted by running a suite of stand-alone Perl executable (PLX) scripts from a MacOS bash terminal command line. The scripts were written and provided by Dr. Kent at the Kent Lab, Cardiff University School of Biosciences Genomics Research Hub for use in creating and processing Kent Lab MNase-seq/Chromatin Particle Sequence Analysis (CPSA) and are accessible under: https://github.com/-chromatin-kent/chromatin_tools.

For plotting paired read insert size (ISIZE) distributions, the script pair_read_histogram.plx was run once for each of the four SAM bio-replicates. This script counts SAM file IDs and tallies a histogram to produce an output file in TXT format. All bio-replicates were processed to 10 000 000 paired reads with an ISIZE boundary of 1000bp and histogram distribution bin width value of 10bp. ISIZE distributions were plotted for each bio-replicate using the $\log_{10}$ paired read frequency (Y axis) against bin width values (X axis). Correlation coefficients were used to test correlation respectively. To map nucleosome distribution on the yeast genome, the script Sc_NC_SAM2_Def_Part_sgr_full.plx was run once for each of the four SAM bio-replicates. This script isolates paired reads of a single specified size

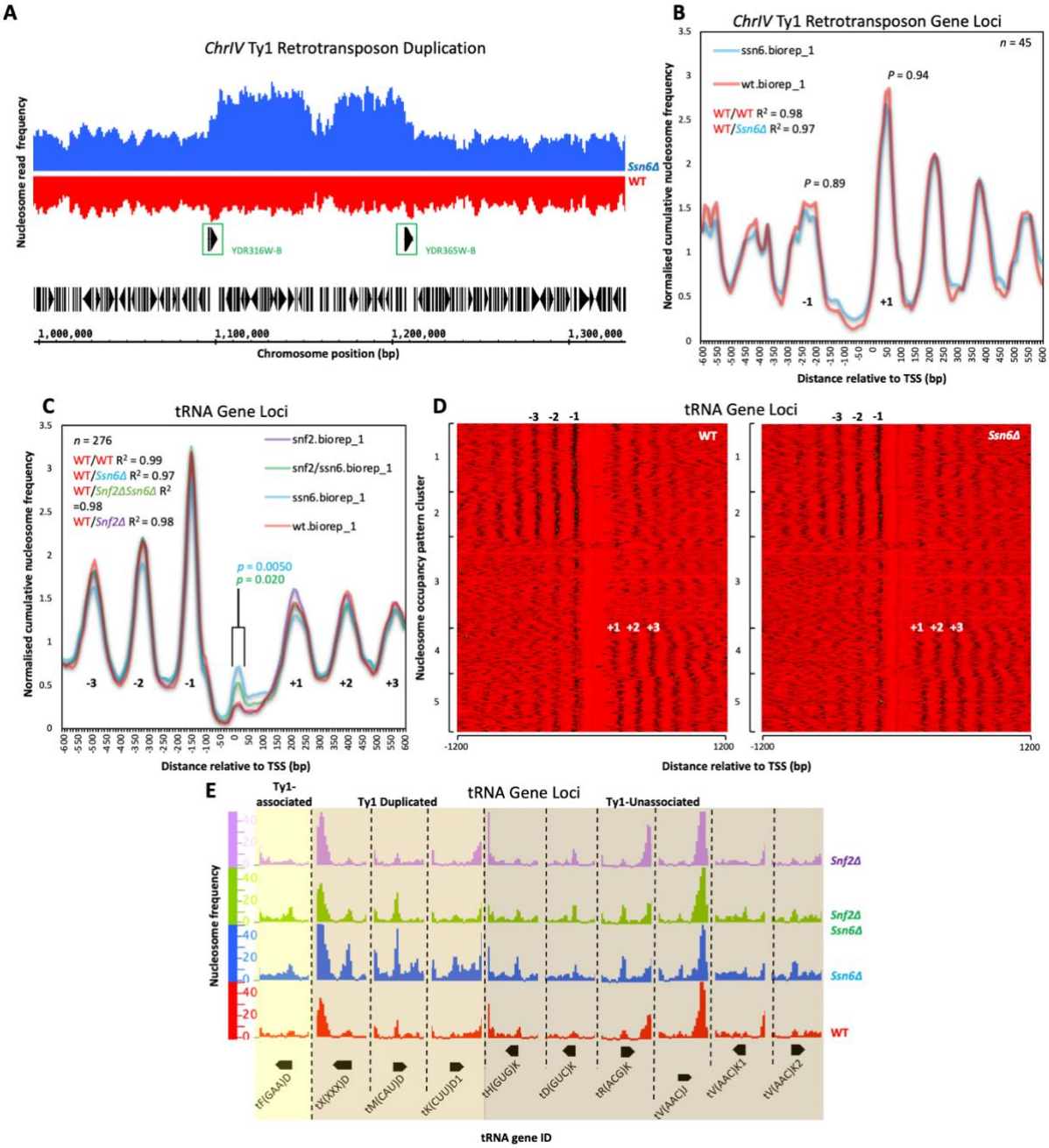

Figure 2 Apparent abnormal *Ssn6Δ ChrIV* nucleosome frequency is due to a Ty1 retrotransposon duplication event that i) results in no change to typical nucleosome occupancy at gene TSSs and ii) could interact with tRNA-encoding gene expression. A Nucleosome frequency is 2.19 times greater within Ty1 transposable elements YDR316-B and YDR365W-B (position chrIV:1 101 332-1 206 996, indicated green) than without. *ChrIV* nucleosome frequency used 1000bp bin width WT and *Ssn6Δ* SGR chromosome distribution files and is displayed using the S288C strain 2011 SacCer 3 genome. **B** Occupancy remains consistent between samples at the duplication despite increased *Ssn6Δ* nucleosome frequency for. Normalised nucleosome CFDs were plotted for WT and *Ssn6Δ* samples relative to TSSs at positions 1 101 332bp – 1 206 996bp (Xu et al. 2009). *n* - values refer to the total count for input feature files. *p* - values refer to the result of a Wilcoxon Rank Sum test comparing WT with *Ssn6Δ* normalised cumulative frequencies at bin values for -1 and +1 nucleosomes. R^2 – values refer to the correlation coefficient for WT/WT and WT/*Ssn6Δ* occupancies. **C** *Ssn6Δ* and *Snf2ΔSsn6Δ* samples show significantly increased typical nucleosome occupancy at tRNA gene TSS NFRs compared with WT. Normalised nucleosome CFDs were plotted relative to TSS (Cherry et al. 2012). *p* - values refer to the results of Welch's T-tests comparing WT with *Ssn6Δ* (blue) and WT with *Snf2ΔSsn6Δ* (green) nucleosome frequency from -10 to 40bp bin values. **D** Gene Cluster 3.0 found five nucleosome occupancy organisation patterns at tRNA gene TSSs for WT and *Ssn6Δ*. *K* – means clustering was successful one time out of ten runs for both samples. Individual features are plotted (y axis) relative to TSSs (x axis) and *Ssn6Δ* was ordered in correspondence to WT clusters. High, medium and low occupancy levels are indicated by green, black and red respectively. **E** Nucleosome distribution reflects typical occupancy at tRNA gene TSSs at loci found unassociated with Ty1 elements (dark) as well as within (medium) and associated with (light) the *ChrIV* Ty1 retrotransposon duplication.

value and, in order to discriminate for chromatin particles that represented nucleosomes, paired reads were set to 150bp. A paired read size percentage 'particle window' was set to 0.2 (20%) and the histogram distribution bin width value was set to 10bp. This script indexes SAM data according to chromosome ID (I – XVIII) and outputs a 10bp resolution genomic nucleosome distribution in SGR format. The SGR chromosome nucleosome distributions for each bio-replicate were visualised in the Integrated Genome Browser (IGB), loaded against the S288C strain 2011 SacCer 3 genome. For further WT and *Ssn6Δ* nucleosome density visualisation on *ChrIV*, Sc_NC_SAM2_Def_Part_sgr_full.plx was run with bin width set to 1000bp. *Snf2Δ* and *Snf2ΔSsn6Δ* datasets were processed as described by student peers Sadie Ash and Henry Shelton of Cardiff University School of Biosciences for further use in this study.

Genomic feature nucleosome occupancy analysis

To determine the typical nucleosome occupancies of WT, *Ssn6Δ*, *Snf2Δ* and *Snf2ΔSsn6Δ* at Ssn6 binding features normalised nucleosome CFDs were plotted for each sample using the script CFD_Plotter.plx. As inputs, the script requires TXT format files containing four columns of genomic feature data (chromosome ID; site ID; site position; strand) as well as SGR format chromosome nucleosome distribution files. As an output, the script generates two columns in TXT format (bin [relative to feature position]; normalised cumulative frequency) that were used for CFD plotting. Ssn6 binding promoter region and global Ssn6 binding region feature data are derived from processed (https://doi.org/10.26208/rykf-6050) and underlying (https://github.com/CEGRcode/2021-Rossi_Nature) data that defines the genome wide chromatin associated protein architecture in *S. cerevisiae* using chromatin immunoprecipitation, exonuclease digestion and DNA sequencing (ChIP–exo/seq) (Rossi et al. 2021). In addition, tRNA gene and Ty1 retrotransposon associated features for CFD input are respectively obtained from the Saccharomyces Genome Database (SGD) (Cherry et al. 2012) and a genome wide survey of *S. cerevisiae* transcript structure and expression (Xu et al. 2009). Further Ty1 long terminal repeat (LTR) features originate from the SGD (Cherry et al. 2012). *K* – means clustering was performed to group subsets of features by shared nucleosome occupancy patterns in Cluster 3.0 (de Hoon et al. 2004) and its output rendered in Tree View 3 (Saldanha 2004). To test the significance of difference in occupied nucleosome peaks between samples, Wilcoxon Rank Sum tests were run using the script CFD_Compare_Stats_basic.plx set to a chromatin particle size of 150bp matching 150bp nucleosome paired read.

RESULTS

MNase-seq bio-replicates are consistent in chromatin particle size, distribution and with input DNA size spectra

Chromatin particle sizes were found for each of the WT and *Ssn6Δ* bio-replicates by plotting paired read ISIZE distributions. For both sample datasets, three $\log_{10}$ frequency distribution peaks identify mono-, di- and tri-nucleosomal particles, corresponding with ISIZEs of 150bp, 300bp and 450bp respectively (Figure 1B). The size distribution qualitatively reflects input MNase-digested DNA size spectra (Figure 1A, 1B). This The 140-150bp bin category (mono-nucleosomes) consistently yielded the highest paired-read frequency across sample bio-replicates. Further, paired-read frequency descends as bin value ascends from mono- to di- to tri-nucleosomes. Qualitatively, bio-replicate ISIZE $\log_{10}$ frequency distribution profiles resemble each other closely within WT and *Ssn6Δ* samples (Figure 1B). Correlation coefficients generated R^2-values of 0.9883 and 0.9952 for WT and *Ssn6Δ* bio-replicates respectively (Figure 1C) and, thus, there is a very strong correlation between bio-replicates of each sample. These data indicate that bio-replicate datasets with quantitative consistency comprise WT and *Ssn6Δ* samples and that sample comparisons can rely on a single bio-replicate for reference.

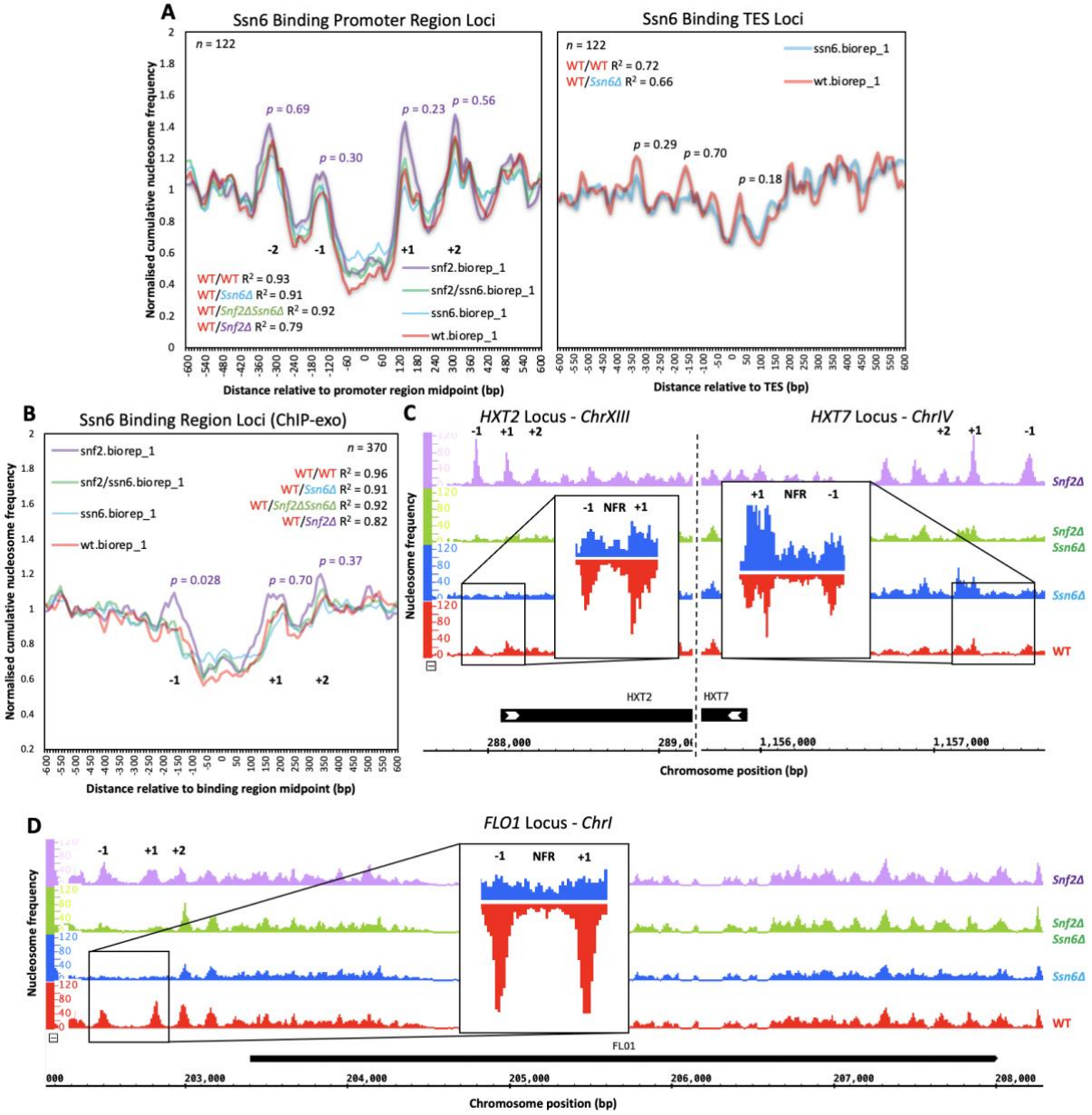

Figure 3 At Ssn6 binding promoter regions, the NFR is typically most accessible in the presence of both Ssn6 and Snf2 while, in the presence of Ssn6 only, significantly stronger -1 nucleosome positioning is observed at Ssn6 binding regions. A For WT, *Ssn6Δ*, *Snf2ΔSsn6Δ* and *Snf2Δ* samples, a NFR and -2, -1, +1 and +2 nucleosomes are generated around the Ssn6 binding promoter region midpoints. Ssn6 binding TESs lack typically positioned nucleosomes. Normalised nucleosome CFDs were plotted for WT, *Ssn6Δ*, *Snf2ΔSsn6Δ* and *Snf2Δ* samples relative to promoter region midpoints and TESs (Rossi et al. 2021). *N* – values refer to the total feature count for promoter and TES input TXT files. *P* – values refer to the result of Wilcoxon Rank Sum tests comparing WT with *Ssn6Δ* (black) and WT with *Snf2Δ* (purple) normalised cumulative frequencies at bin values for -2 to +2 nucleosomes and potential nucleosome peaks for promoter regions and TESs respectively. **B** For *Snf2Δ*, the -1 nucleosome is significantly more strongly positioned that for WT at Ssn6 binding regions while WT, *Ssn6Δ*, *Snf2ΔSsn6Δ* and *Snf2Δ* samples NFR accessibility is ordered in consistence with Ssn6 binding promoter regions. Normalised nucleosome CFDs were plotted for WT and *Ssn6Δ* samples relative to binding region midpoints (Rossi et al. 2021). *N* – values refer to the total feature count for the ChIP-exo binding region input file. *P* – values refer to the result of Wilcoxon Rank Sum tests comparing WT with *Snf2Δ* normalised cumulative frequencies at bin values for -1 to +2 nucleosomes.**C** *HXT2* and *HXT7* promoter regions nucleosome distributions reflect typical -1 to +2 nucleosome occupancy and NFR accessibility at Ssn6 binding regions (ChIP-exo) and promoter regions respectively. **D** At the *FLO1* promoter region, -1 to +2 nucleosome frequency is reduced compared with *HXT2 and HXT7* loci and reflects typical occupancy and NFR accessibility at Ssn6 binding regions (ChIP-exo) and promoter regions to a lesser extent.

Abnormal Ssn6Δ nucleosome sequence read frequency by Ty1 retrotransposon duplication

The distribution of nucleosomes over chromosomal regions was visualised by plotting 150bp sized MNase-seq read frequency distributions. Peaks were manually catalogued for qualitative comparisons. *ChrII SSN6* (*CYC8*) locus deletion was confirmed in the *Ssn6Δ* strain (Figure 1D). Building on their quantitative consistency, bio-replicates lacked notable visual discrepancies in each sample. As a result, only wt.biorep_1.sgr and ssn6Δ.biorep_1.sgr files were subject to further downstream analyses. Apparently abnormal nucleosome frequency was detected in *Ssn6Δ* spanning a ~1kbp region (position chrIV:1 101 332-1 206 996) (Figure 2A), flanked downstream and upstream by gag-pol fusion genes YDR316W-B (NCBI RefSeq accession no. NM_001184425.2) and YDR365W-B (NCBI RefSeq accession no. NM_001184427.2) respectively. Gag-pol fusions indicate yeast polyprotein-encoding retrotransposon genes capable of DNA element transposition in a recombination event (Kim et al. 1998; Lesage and Todeschini 2005). In particular, YDR316W-B and YDR365W-B are known Ty1 retrotransposon elements. To test the nucleosome density of the region, mean nucleosome frequencies were calculated for two 10.4kbp regions: chrIV:1 102 000-1 206 000 (representing the abnormal region) and chrIV:1 210 000-1 314 000 (proxy for normal *chrIV* frequency estimation). The normal mean *chrIV* frequency was estimated at 1359 while the abnormal region yielded 2981, increasing by a factor of 2.19. At approximately double the expected and taken together with its Ty1 element association, abnormal *chrIV* nucleosome frequency suggests a Ty1 retrostransposon recombination event leading to the regions MNase-digested sequence read duplication.

Typical tRNA gene nucleosome occupancy reflects Ty1 retrotransposon duplication

The transcript abundance of Ty1 elements is known to be influenced by active tRNA-encoding genes (Bolton and Boeke 2003) and, likewise, tRNA gene transcriptional activity can show dependance on the association with a particular Ty element (Nelbock et al. 1985; Krieg et al. 1991; Hani and Feldmann 1998). In order to understand how Ty1 duplication occurred in *Ssn6Δ*, typical nucleosome occupancy was determined for TSSs at positions chrIV:1 101 332-1 206 996 (Figure 2B), global Ty1 long-terminal repeats (LTRs) (Appendix Figure 1A) and global tRNA TSSs (Figure 2C). As such, it was suspected that Ssn6 could have a role in the interplay between Ty1 retrotransposons and tRNA genes.

For typical nucleosome occupancy analysis at the *chrIV* Ty1 retrotransposon duplication, 45 TSSs (21 forward, 24 reverse) were confirmed from 48 gene IDs positioned between 1 101 332bp and 1 206 996bp. Despite an approximately two-fold increase in nucleosome frequency in the region, occupancy at -1 and +1 nucleosomes is not significantly different between samples (Figure 2B). Samples with R^2 - value coefficients of 0.61-0.80, 0.81-0.90, 0.91-0.95 and 0.96-1.0 are said to correlate weakly, intermediately, strongly and very strongly, respectively. WT and *Ssn6Δ* correlated very strongly and to a similar degree as WT bio-replicates. A total of 266 Ty1 LTRs (21 forward, 24 reverse) were analyzed and, globally, occupancy at -1 and +1 nucleosomes is not significantly different between samples, achieving $p = 0.97$ and $p = 0.64$ in Wilcoxon Ranked Sum tests respectively (Appendix Figure 1A). Correlation coefficients were found at $R^2 = 0.86$ and $R^2 = 0.89$ between WT bio-replicates and WT and *Ssn6Δ* respectively. Taken together, these results indicate that global Ty1 LTR and Ty1 retrotransposon (chrIV: 1 101 332-1 206 996) typical nucleosome occupancy is similarly unaffected by *Ssn6* deletion. As such, the *ChrIV* Ty1 retrotransposon duplication is not attributed to direct Ssn6-Tup1 remodeling activity at Ty1 LTR regions or TSSs at the element.

In order to test whether Ty1 retrotransposon duplication was the result of a loss of Ssn6-remodeling-mediated tRNA gene transcription modulation, typical nucleosome occupancy was determined for 276 (143 forward, 132 reverse) confirmed tRNA gene TSSs. For all mutants (*Ssn6Δ*, *Snf2Δ* and *Snf2ΔSsn6Δ*), occupancies correlated very strongly with wt.biorep_1 (lowest at $R^2 = 0.97$ for WT/*Ssn6Δ*) and to a similar degree as wt.biorep_2. Significantly stronger occupancy was observed in *Ssn6Δ* and *Snf2ΔSsn6Δ* than in WT at the -10bp to 40bp peak position (Figure 2C). To visualize the organization of nucleosome occupancy at individual features and to understand whether a subset of

tRNA gene loci contributed to the -10bp to 40bp peak in *Ssn6Δ*, nucleosome organization patterns were determined through *k* – means clustering. Clustered individually, nucleosomes of low to medium occupancy levels were positioned cluster-wide corresponding with the -10bp to 40bp occupancy peak in both WT and *Ssn6Δ*. Nucleosome organization from -100 to 150bp across all WT and *Ssn6Δ* patterns reflected their samples respective typical occupancy (Figure 2D, 2C, Appendix Figure 1B). Thus, stronger typical occupancy at the -10bp to 40bp peak in *Ssn6Δ* is not attributed to any clustering subset of tRNA gene loci and, as the feature composition of pattern clusters is almost identical, WT and *Ssn6Δ* patterns were ordered identically for organizational comparison. Nucleosomes -3, -2, -1 and +1, +2, +3 in clusters 1, 2 and 4, 5 respectively correspond with typical tRNA gene occupancy in WT and in *Ssn6Δ* (Figure 2C, 2D). Finally, the genomic position of exemplar tRNA gene loci with nucleosome distributions representing typical nucleosome occupancy in WT, *Ssn6Δ*, *Snf2Δ* and *Snf2ΔSsn6Δ* is not limited to the *chrIV* Ty1 retrotransposon duplication (Figure 2E). A sample of six tRNA genes unassociated with Ty1 elements were identified with distributions reflecting typical occupancy.

Swi/Snf and Ssn6-Tup1 co-occupancy is required for full NFR formation at Ssn6 promoter region targets

Ssn6 organizes nucleosome positioning into repressive chromatin states in a corepressor complex with Tup1 at subsets of loci including *FLO1*, *SUC2* and *RNR3* gene promoter regions (Fleming and Pennings 2007; Fleming et al. 2014). In order to understand the Ssn6-Tup1/Swi-Snf remodeling interplay at features with Ssn6 activity, typical nucleosome occupancy at SSN6 binding promoter regions, TESs (Figure 3A) and ChIP-exo region loci (Figure 3B) was determined. At 122 (67 forward, 55 reverse) promoter regions bound by Ssn6, -2 to +2 nucleosomes formed in WT, *Ssn6Δ*, *Snf2Δ* and *Snf2ΔSsn6Δ* samples with an NFR at the midpoint (Figure 3A). Wilcoxon Rank Sum tests found the difference in occupancy strength for *Snf2Δ* and WT nucleosomes to not be significant. Occupancies suggest *Ssn6Δ* and WT samples typically contain the most and least accessible NFRs respectively. All comparisons correlated strongly, except WT with *Snf2* which are weakly correlated. For 122 (67 forward, 55 reverse) TESs bound by Ssn6, three potential nucleosome peaks are not significantly different between WT and *Ssn6Δ* samples while both occupancy comparisons correlate weakly (Figure 3A).

Across 370 (370 forward) Ssn6 binding regions (ChIP-exo), WT, *Ssn6Δ*, *Snf2Δ* and *Snf2ΔSsn6Δ* NFR accessibility is in accordance with that of SSN6 binding promoter regions (Figure 3B, 3A). However, typical nucleosome occupancy at ChIP-exo Ssn6 binding regions is in contrast with Ssn6 binding promoter regions by a lack of -1 and +2 nucleosomes for WT, *Ssn6Δ* and *Snf2ΔSsn6Δ* as well as significantly stronger -1 nucleosome occupancy for *Snf2Δ* than WT (Figure 3B). Comparisons by correlation coefficients consolidate the typical occupancy differences between samples at ChIP-exo Ssn6 binding regions but correspond with sample occupancy correlations at Ssn6 binding promoter regions.

'Main' hexose transporter genes *HXT2* and *HXT7* (Nijland et al. 2017) were used as model loci as their respective nucleosome distributions reflect typical Ssn6 binding promoter region and global ChIP-exo region nucleosome occupancy for WT, *Ssn6Δ*, *Snf2Δ* and *Snf2ΔSsn6Δ* samples (Figure 3C). Nucleosome frequencies at *HXT2* and *HXT7* NFRs are found to increase by a factor of 1.32 and 3.15 from WT to *Ssn6Δ* respectively. In order to test whether the *HXT2* and *HXT7* loci could belong to the subset of genes robustly repressed by Ssn6 nucleosome remodeling activity, *FLO1* promoter nucleosome distribution was examined. At the *FLO1* promoter, NFR nucleosome frequency increased by a factor of 1.52 from WT to *Ssn6Δ* respectively, corresponding with *HXT2* and *HXT7* loci. While nucleosome positioning and NFR accessibility at the *FLO1* locus reflects typical Ssn6 binding promoter region occupancy, the *HXT2* and *HXT7* loci are in accordance with typical ChIP-exo binding region -1 nucleosome strength.

DISCUSSION

The MNase-seq S. cerevisiae nucleosome landscape on informing eukaryote genome regulation

Chromatin structure remodeling by altering nucleosome positioning throughout the genome is a central mechanism of gene expression regulation in all eukaryotes. Nuclease-digested DNA fragment sequences obtained from a given strain and aligned with the SacCer 3 genome provide the genomic landscape of *S. cerevisiae* nucleosomes. Here, MNase-seq paired reads from *SSN6*, *SNF2* and *SSN6*/*SNF2* mutant strain samples are offer an insight into the effect of co-occupying chromatin remodeling interactions between Swi/Snf and Ssn6-Tup1 complexes on gene expression at loci binding Ssn6.

Consistency in bio-replicate paired read size distributions among samples and their reflection of input DNA size spectra confirms that the data here shows chromatin particles ranging from mono- to tri-nucleosomes in a manner accurate enough for subsequent nucleosome occupancy analyses. This result reinforces the utility of MNase-seq directed nucleosome arrangement and occupancy analyses in understanding chromatin remodeling mechanisms as the data represents the fundamental unit of chromatin structures. The visualization of *SSN6* deletion further evidences the accuracy of 150bp nucleosome paired reads in relation to genomic position.

Swi/Snf and Ssn6-Tup1 chromatin remodeling in Ty1 retrotransposon modulated tRNA gene expression

The detection of a Ty1 retrotransposon duplication event initially highlights a disparity in precision between the biochemical and bioinformatic aspects to understanding genome regulation. While differential nucleosome density associated with lack of Ssn6 chromatin remodeling activity at the retrotransposon could be informative, the potential for recombination and integration throughout the genome during culturing detracts from the validity of inferences relating to nucleosome occupancy at the Ty-1 retrotransposon (*chrIV*: 1 101 332bp – 1 206 996bp). Indeed,

Initially, it was considered that Swi/Snf and Ssn6-Tup1 alter nucleosome positioning into a repressive chromatin state at Ty1 elements causing their transcriptional downregulation and blocking their transposition. The evidence to suggest the complexes do not carry out this role is twofold: i) Typical nucleosome occupancy at Ty1 LTR loci is consistent between WT and *Ssn6Δ* samples ii) At the *chrIV* Ty1 retrotransposon, occupancy around gene TSSs is consistent between WT and *Ssn6Δ* samples despite 2.19 times higher nucleosome frequency ii) The *Ssn6Δ* Ty1 retrotransposon duplication on *chrIV* does not occur in WT, *Snf2Δ* or *Snf2ΔSsn6Δ* samples. Further, (ii) builds on the finding that the abnormal frequency is due to a duplication of DNA and, together with (ii), provides evidence against a chromatin remodeling role for Swi/Snf and Ssn6-Tup1 complexes in Ty1 element expression and transposition.

S. cerevisiae tRNA gene and Ty1 element interactions are known to be based on their relative positioning in the genome. Ty1 element insertions interfere with RNA polymerase III (pol III) transcribed genes such as those encoding tRNAs (the preferred Ty1 integration targets), exerting a neutral to modest stimulatory effect on gene expression (Bolton and Boeke 2003). In addition, Ty1 element association with several tRNA genes is known to influence tRNA transcriptional activity (Hani and Feldmann 1998). The bidirectionally organized association between tRNA gene tF(GAA)D and Ty1 element YDR316W-B supports the latter route of Ty1 retrotransposon duplication (Figure 2E). However, as Ty1 duplication is not seen in *Snf2ΔSsn6* yet similarly positioned nucleosomes occupy the samples tRNA gene NFRs as in *Ssn6Δ*, Ty1 element interference with tRNA gene expression by retrotransposon insertion or organizational associated is not solely attributed tRNA gene nucleosome occupancies in this study. The data suggest that Ssn6-Tup1 creates a typically more open chromatin state at these tRNA gene NFRs and the greater extent to which nucleosomes are positioned at the TSS

in *Ssn6Δ* than in *Snf2ΔSsn6Δ* could reflect duplicated tRNA gene loci found on the *chrIV* Ty1 retrotransposon as well as the unknown targets of Ty1 insertion. However, as the data show only DNA that is wrapped by nucleosomes aligned to the *S. cerevisiae* genome, this study lacks the scope to determine at which genomic positions the duplicated DNA is inserted. Thus, the targets of Ty1 insertion are not identified and the degree to which Ty1 integration associated with tRNA gene loci effects tRNA gene NFR nucleosome positioning is not certain.

The Ty1 retrotransposon DNA duplicating recombination event occurs during *S. cerevisiae* culturing that prevents accurate mapping of the nucleosome landscape at the region. It is suggested that a series of repeat *Ssn6Δ* strain culturing would clarify the reproducibility of this genomic instability and its interaction via nucleosome positioning with tRNA gene loci. By studying insertion sites of sequence tagged Ty1 elements, the extent to which Ty1 insertion interactions with tRNA gene loci result in positioned nucleosomes at the NFR compared with Ssn6-Tup1 tRNA gene NFR remodeling could be elucidated further.

Co-occupying Swi/Snf and Ssn6-Tup1 remodel chromatin into a transcriptionally activating state at promoter region NFRs targeted by Ssn6

While Fleming and Pennings (2007) highlight the long-range remodelling of chromatin structure domains upstream from the *SUC2* promoter by Ssn6-Tup1, the typical nucleosome occupancy data in this study capture local remodelling at promoter region NFRs to generate more open chromatin states in Swi/Snf and Ssn6-Tup1 co-occupancy. As such, the data suggest co-occupying remodelling interactions between these two complexes results in the most open NFR chromatin structure generating increased DNA binding accessibility. Promoter region NFRs are greatly enriched for DBP binding sites including the TATA-box and a range of transcription factor binding motifs (Sun et al. 2009). Given the significance of these binding sites to transcriptional regulation, factors that modulate chromatin structure accessibility at NFRs by remodelling at the nucleosome level are likely to positively or negatively regulate gene expression. Thus, co-occupying Swi/Snf and Ssn6-Tup1 are suggested to maintain open NFRs that facilitate the binding of transcription machinery such as RNA Pol II and sequence specific transcription factors.

Here, typical nucleosome occupancy data support a co-activating role for Ssn6-Tup1 in co-occupancy with Swi/Snf at Ssn6 binding promoter regions (Figure 3A, 3B) (Fleming and Pennings 2007; Fleming et al. 2014). Ssn6-Tup1 remodelling activity alone forms modestly to significantly repressive chromatin structures, generating well positioned -2 to +2 nucleosomes around promoter region NFRs and significantly positioned -1 nucleosomes across all binding region loci (Figure 3A, 3B). Taken together, these findings are partly at odds with general co-repressor roles of Ssn6-Tup1 (Parnell and Stillman 2011) by providing evidence for Swi/Snf dependant Ssn6-Tup1 remodelling with transcriptionally co-activating effects on chromatin structure accessibility. Importantly, processed and underlying chromatin associated protein architecture data (Rossi et al. 2021) are demonstrated as feature sources for determining the individual and co-occupying effects on nucleosome occupancy and positioning of remodelling complexes such as Swi/Snf and Ssn6-Tup1. The -2 nucleosome positioning discrepancy between ChIP-exo Ssn6 binding regions and Ssn6 binding promoter regions reflects the range of features that comprise each. Although the ultimate influence of Ssn6-Tup1 and its remodelling interactions with Swi/Snf on gene expression regulation is most relevant at promoter regions, Ssn6 binding is not limited to such regions (Figure 1A). Features such as TESs increase nucleosome noise in typical occupancies highlighting the broad and generalised view that CFD plots of typical occupancy acquire of the nucleosome landscape. Further, while sample-wide resemblance in occupancy correlation and NFR accessibility between Ssn6 binding promoter regions and ChIP-exo Ssn6 binding regions indicate Ssn6 binding regions comprise largely of promoter regions, only *Snf2Δ* -1 nucleosome occupancy is significantly higher than in WT. This

also indicates the range of genomic features that contribute to ChIP-exo Ssn6 binding regions and their subsequent typical chromatin structure.

Swi/Snf and Ssn6-Tup1 co-occupancy at HXT2 and HXT7 promoters demonstrates nuanced opposed remodelling interplay despite Ssn6-Tup1 repression

Chen et al. (2013) fount that, after mobilisation by Isw2, *HXT8* promoter nucleosomes positioned in the NFR (likely previously undetected due to low occupancy) may be locked by Ssn6-Tup1 and blocking the TATA-box. In this way, gene expression is negatively regulated by repressive Ssn6-Tup1 chromatin remodelling at NFRs. The finding that nucleosome distributions *HXT2* and *HXT7* promoter region NFRs reflect typical nucleosome occupancies at Ssn6 binding promoter regions and ChIP-exo regions is partially contradictory to the notion of repressive Ssn6-Tup1 remodelling at hexose transporter encoding gene promoter NFRs. Indeed, Ssn6-Tup1 activity generates well positioned *HXT2* -1 and +1 nucleosomes indicative of a repressive chromatin structure at the locus, but Swi/Snf and Ssn6-Tup1 co-occupying remodelling appears to also facilitate more accessible NFRs for *HXT2* and *HXT7* loci. In this way, the complexes interact to balance their individual chromatin structure remodelling activity. Further, this chromatin structure is at odds with the *FLO1* promoter region NFR which is consistent with work finding its robust repression by Ssn6-Tup1 (Fleming et al. 2014). Further, Ssn6-Tup1 is able to raise the extent to which -1 and +1 nucleosomes are positioned to form a transcriptionally repressive chromatin structure at the *HXT2* and *HXT7* in the absence of Swi/Snf.

Previous studies on Ssn6-Tup1 investigate the complexes transcriptionally repressive chromatin structure remodelling at long range and local as well as individual and co-occupying levels (Fleming and Pennings 2007; Fleming et al. 2014; Nijland et al. 2017). Typical nucleosome occupancy data here provide evidence for competing positive and negative regulatory roles of Swi/Snf and Ssn6-Tup1 co-occupying remodelling interactions at the 'main' hexose transporter encoding genes. This presents an interplay of compromise between the complexes where the sum effect of their combined activity on nucleosome landscapes is more nuanced than their co-activator and co-repressor classifications. In particular, the *HXT2* locus is a snapshot of balancing remodelling effects on chromatin structure where overall chromatin structure is transcriptionally repressive yet Swi/Snf and Ssn6-Tup1 co-occupancy mediated NFR accessibility is evident.

APPENDICES

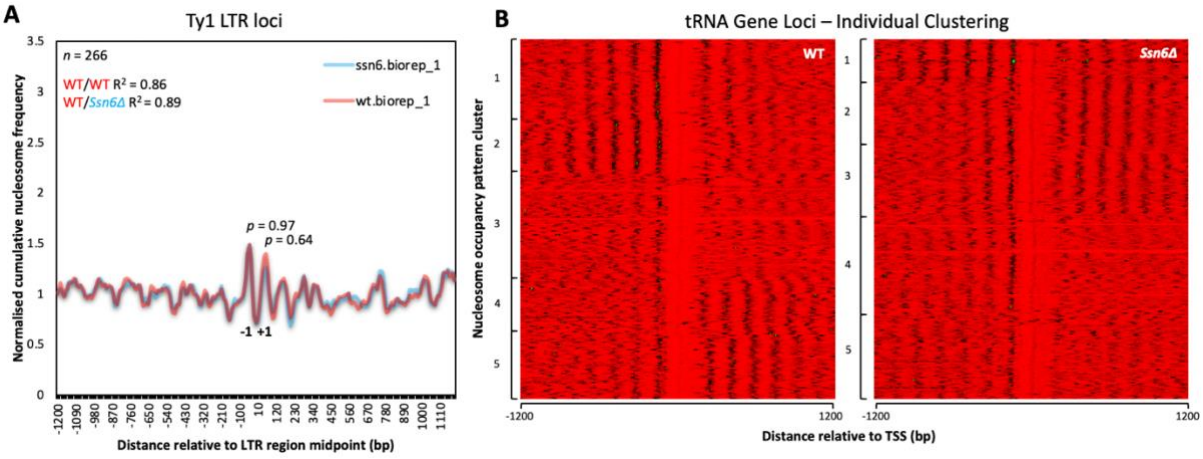

Appendix Figure 1 *ChrIV* Ty1 retrotransposon duplication event is not the result of altered Ty1 LTR and no subset of tRNA gene loci are attributed to typical nucleosome occupancy across tRNA gene. A Typical nucleosome occupancy among Ty1 LTR loci remains consistent for WT and *Ssn6Δ* and Ssn6-Tup1 chromatin structure remodelling is not observed. Normalised nucleosome CFDs were plotted for WT and *Ssn6Δ* samples relative to LTR region midpoints. *N* – values refer to the total feature count for LTR input TXT files. *P* – values refer to the result of Wilcoxon Rank Sum tests comparing WT with *Ssn6Δ* normalised cumulative frequencies at bin values for -1 to +1nucleosomes. **B** Gene Cluster 3.0 found five nucleosome occupancy organisation patterns at tRNA gene TSSs for WT and *Ssn6Δ* individually. *K* – means clustering was successful one time out of ten runs for both samples. Individual features are plotted (y axis) relative to TSSs (x axis). High, medium and low occupancy levels are indicated by green, black and red respectively.

References

Bolton, E. C. and Boeke, J. D. 2003. Transcriptional interactions between yeast tRNA genes, flanking genes and Ty elements: a genomic point of view. *Genome Res* 13(2), pp. 254-263. doi: 10.1101/gr.612203

Chen, K. et al. 2013. Stabilization of the promoter nucleosomes in nucleosome-free regions by the yeast Cyc8-Tup1 corepressor. *Genome Res* 23(2), pp. 312-322. doi: 10.1101/gr.141952.112

Cherry, J. M. et al. 2012. Saccharomyces Genome Database: the genomics resource of budding yeast. *Nucleic Acids Res* 40(Database issue), pp. D700-705. doi: 10.1093/nar/gkr1029

Courey, A. J. and Jia, S. 2001. Transcriptional repression: the long and the short of it. *Genes Dev* 15(21), pp. 2786-2796. doi: 10.1101/gad.939601

de Hoon, M. J., Imoto, S., Nolan, J. and Miyano, S. 2004. Open source clustering software. *Bioinformatics* 20(9), pp. 1453-1454. doi: 10.1093/bioinformatics/bth078

Eisen, J. A., Sweder, K. S. and Hanawalt, P. C. 1995. Evolution of the SNF2 family of proteins: subfamilies with distinct sequences and functions. *Nucleic Acids Res* 23(14), pp. 2715-2723. doi: 10.1093/nar/23.14.2715

Fleming, A. B., Beggs, S., Church, M., Tsukihashi, Y. and Pennings, S. 2014. The yeast Cyc8-Tup1 complex cooperates with Hda1p and Rpd3p histone deacetylases to robustly repress transcription of the subtelomeric FLO1 gene. *Biochim Biophys Acta* 1839(11), pp. 1242-1255. doi: 10.1016/j.bbagrm.2014.07.022

Fleming, A. B. and Pennings, S. 2007. Tup1-Ssn6 and Swi-Snf remodelling activities influence long-range chromatin organization upstream of the yeast SUC2 gene. *Nucleic Acids Res* 35(16), pp. 5520-5531. doi: 10.1093/nar/gkm573

Hani, J. and Feldmann, H. 1998. tRNA genes and retroelements in the yeast genome. *Nucleic Acids Res* 26(3), pp. 689-696. doi: 10.1093/nar/26.3.689

Havas, K., Flaus, A., Phelan, M., Kingston, R., Wade, P. A., Lilley, D. M. and Owen-Hughes, T. 2000. Generation of superhelical torsion by ATP-dependent chromatin remodeling activities. *Cell* 103(7), pp. 1133-1142. doi: 10.1016/s0092-8674(00)00215-4

Hirschhorn, J. N., Brown, S. A., Clark, C. D. and Winston, F. 1992. Evidence that SNF2/SWI2 and SNF5 activate transcription in yeast by altering chromatin structure. *Genes Dev* 6(12A), pp. 2288-2298. doi: 10.1101/gad.6.12a.2288

Kent, N. A., Adams, S., Moorhouse, A. and Paszkiewicz, K. 2011. Chromatin particle spectrum analysis: a method for comparative chromatin structure analysis using paired-end mode next-generation DNA sequencing. *Nucleic Acids Res* 39(5), p. e26. doi: 10.1093/nar/gkq1183

Kent, N. A. and Mellor, J. 1995. Chromatin structure snap-shots: rapid nuclease digestion of chromatin in yeast. *Nucleic Acids Res* 23(18), pp. 3786-3787. doi: 10.1093/nar/23.18.3786

Kim, J. M., Vanguri, S., Boeke, J. D., Gabriel, A. and Voytas, D. F. 1998. Transposable elements and genome organization: a comprehensive survey of retrotransposons revealed by the complete Saccharomyces cerevisiae genome sequence. *Genome Res* 8(5), pp. 464-478. doi: 10.1101/gr.8.5.464

Krieg, R., Stucka, R., Clark, S. and Feldmann, H. 1991. The use of a synthetic tRNA gene as a novel approach to study in vivo transcription and chromatin structure in yeast. *Nucleic Acids Res* 19(14), pp. 3849-3855. doi: 10.1093/nar/19.14.3849

Langmead, B., Trapnell, C., Pop, M. and Salzberg, S. L. 2009. Ultrafast and memory-efficient alignment of short DNA sequences to the human genome. *Genome Biol* 10(3), p. R25. doi: 10.1186/gb-2009-10-3-r25

Lesage, P. and Todeschini, A. L. 2005. Happy together: the life and times of Ty retrotransposons and their hosts. *Cytogenet Genome Res* 110(1-4), pp. 70-90. doi: 10.1159/000084940

Li, H. et al. 2009. The Sequence Alignment/Map format and SAMtools. *Bioinformatics* 25(16), pp. 2078-2079. doi: 10.1093/bioinformatics/btp352

Logie, C. and Peterson, C. L. 1997. Catalytic activity of the yeast SWI/SNF complex on reconstituted nucleosome arrays. *EMBO J* 16(22), pp. 6772-6782. doi: 10.1093/emboj/16.22.6772

Malave, T. M. and Dent, S. Y. 2006. Transcriptional repression by Tup1-Ssn6. *Biochem Cell Biol* 84(4), pp. 437-443. doi: 10.1139/o06-073

Mittal, P. and Roberts, C. W. M. 2020. The SWI/SNF complex in cancer - biology, biomarkers and therapy. *Nat Rev Clin Oncol* 17(7), pp. 435-448. doi: 10.1038/s41571-020-0357-3

Nelbock, P., Stucka, R. and Feldmann, H. 1985. Different patterns of transposable elements in the vicinity of tRNA genes in yeast: a possible clue to transcriptional modulation. *Biol Chem Hoppe Seyler* 366(11), pp. 1041-1051. doi: 10.1515/bchm3.1985.366.2.1041

Nijland, J. G., Shin, H. Y., Boender, L. G. M., de Waal, P. P., Klaassen, P. and Driessen, A. J. M. 2017. Improved Xylose Metabolism by a CYC8 Mutant of Saccharomyces cerevisiae. *Appl Environ Microbiol* 83(11), doi: 10.1128/AEM.00095-17

Parnell, E. J. and Stillman, D. J. 2011. Shields up: the Tup1-Cyc8 repressor complex blocks coactivator recruitment. *Genes Dev* 25(23), pp. 2429-2435. doi: 10.1101/gad.181768.111

Rossi, M. J. et al. 2021. A high-resolution protein architecture of the budding yeast genome. *Nature* 592(7853), pp. 309-314. doi: 10.1038/s41586-021-03314-8

Saldanha, A. J. 2004. Java Treeview--extensible visualization of microarray data. *Bioinformatics* 20(17), pp. 3246-3248. doi: 10.1093/bioinformatics/bth349

Sudarsanam, P., Iyer, V. R., Brown, P. O. and Winston, F. 2000. Whole-genome expression analysis of snf/swi mutants of Saccharomyces cerevisiae. *Proc Natl Acad Sci U S A* 97(7), pp. 3364-3369. doi: 10.1073/pnas.050407197

Sun, W., Xie, W., Xu, F., Grunstein, M. and Li, K. C. 2009. Dissecting nucleosome free regions by a segmental semi-Markov model. *PLoS One* 4(3), p. e4721. doi: 10.1371/journal.pone.0004721

Tsukiyama, T. 2002. The in vivo functions of ATP-dependent chromatin-remodelling factors. *Nat Rev Mol Cell Biol* 3(6), pp. 422-429. doi: 10.1038/nrm828

Venkatesh, S. and Workman, J. L. 2015. Histone exchange, chromatin structure and the regulation of transcription. *Nat Rev Mol Cell Biol* 16(3), pp. 178-189. doi: 10.1038/nrm3941

Voong, L. N., Xi, L., Wang, J. P. and Wang, X. 2017. Genome-wide Mapping of the Nucleosome Landscape by Micrococcal Nuclease and Chemical Mapping. *Trends Genet* 33(8), pp. 495-507. doi: 10.1016/j.tig.2017.05.007

Wach, A., Brachat, A., Pohlmann, R. and Philippsen, P. 1994. New heterologous modules for classical or PCR-based gene disruptions in Saccharomyces cerevisiae. *Yeast* 10(13), pp. 1793-1808. doi: 10.1002/yea.320101310

Whitehouse, I., Flaus, A., Cairns, B. R., White, M. F., Workman, J. L. and Owen-Hughes, T. 1999. Nucleosome mobilization catalysed by the yeast SWI/SNF complex. *Nature* 400(6746), pp. 784-787. doi: 10.1038/23506

Winston, F. and Carlson, M. 1992. Yeast SNF/SWI transcriptional activators and the SPT/SIN chromatin connection. *Trends Genet* 8(11), pp. 387-391. doi: 10.1016/0168-9525(92)90300-s

Xu, Z. et al. 2009. Bidirectional promoters generate pervasive transcription in yeast. *Nature* 457(7232), pp. 1033-1037. doi: 10.1038/nature07728